CHALMERS
UNIVERSITY OF TECHNOLOGY

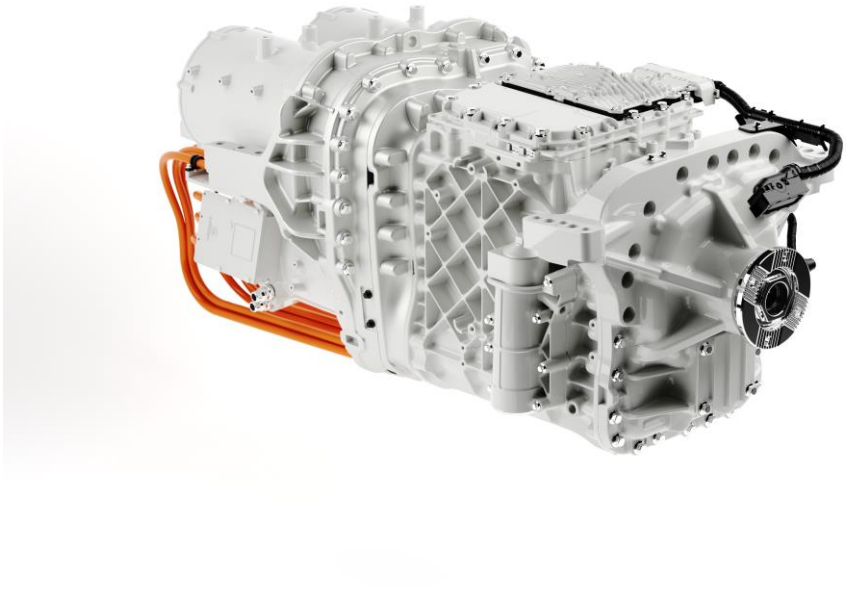

FEM Simulation of Acoustic Radiation from Electric Drivelines in Heavy Trucks

Master's thesis in Applied Mechanics

Monika Stoyanova

Department of Mechanics and Maritime Sciences

CHALMERS UNIVERSITY OF TECHNOLOGY
Gothenburg, Sweden 2022
www.chalmers.se

MASTER'S THESIS IN APPLIED MECHANICS

FEM Simulation of Acoustic Radiation from Electric Drivelines in Heavy Trucks

MONIKA STOYANOVA

Department of Mechanics and Maritime Sciences
Division of Dynamics
CHALMERS UNIVERSITY OF TECHNOLOGY
Göteborg, Sweden 2022

FEM Simulation of Acoustic Radiation from Electric Drivelines in Heavy Trucks

MONIKA STOYANOVA

Supervisors: Anders Frid, Ph.D. Group manager CAE Dynamics and vibration, AFRY
Martina Andersson, Simulation Engineer, Volvo Group Trucks Technology
Sven Norberg, Simulation Engineer, Volvo Group Trucks Technology

Examiner: Håkan Johansson, Professor at Mechanics and Maritime Sciences,
Division of Dynamics, Chalmers University of Technology

Master's thesis 2022:08
Department of Mechanics and Maritime Sciences
Division of Dynamics
Chalmers University of Technology
SE-412 96 Göteborg
Sweden
Telephone: + 46 (0)317721000

Cover:
Electric driveline of a heavy truck, retrieved with permission from Volvo Trucks Media Library.

Department of Mechanics and Maritime Sciences
Göteborg, Sweden 2022

Abstract

Switching from conventional drivelines to electric drivelines in heavy trucks is a crucial step in the development towards a more sustainable transportation. However, with this change the noise emitted from a vehicle is more tonal compared to the broad-spectrum noise from a vehicle with a combustion engine, which can in some situations be perceived as disturbing. Therefore, it is of interest to study and reduce the noise emission from electric drivelines. In this thesis, the main goal is to develop an efficient method based on finite element method (FEM) to simulate the noise emission from an electric drive unit (EDU) during excitation using the commercial software Abaqus.

Using structural-acoustic interaction in Abaqus, the electric drive unit is coupled to the exterior acoustic domain (air) which enables to solve the forward-coupled structural-acoustic problem. To simulate the noise emission in terms of sound pressure, sound intensity, and sound power, direct-solution steady-state dynamic analysis is performed. The obtained acoustic quantities are extracted and further post-processed to be presented in decibel scale (dB).

A monopole source was created to verify the employed simulation method by comparing the acoustic pressure to a theoretical value for a spherical geometry of the monopole source. The results from the simulation and the theoretical expression showed a strong correlation which indicates that the modelling of the structural-acoustic interface works properly. This applies also that the electric drive unit couples correctly to the acoustic domain modelled in this thesis.

Furthermore, the acoustic boundary conditions were verified by comparing a sphere with non-reflective surface and a hemisphere with no reflection on the surface of the cap and total reflection on the ground of the hemisphere. When comparing a sphere with a hemisphere with the above-mentioned boundary conditions, the expectations are to obtain the same sound power. Running the simulations resulted in the same sound power which means that the boundary conditions are applied correctly.

Using the commercial software Abaqus, the forward-coupled structural-acoustic problem can be solved. Both, direct-solution steady-state dynamic analysis and modal-based steady-state dynamic analysis were performed. One of the conclusions that can be drawn is that the direct-solution is more appropriate for solving the exterior acoustic problem than the modal-based solution since it shows a reasonable behavior approaching higher frequencies.

Sammanfattning

Ett viktigt steg i utvecklingen mot hållbara transporter är att ersätta konventionella drivlinor med elektriska drivlinor i tunga lastbilar. I samband med denna övergång blir ljudet från fordonen mer tonalt jämfört med ett brett ljudspektrum för en förbränningsmotor. Detta resulterar i att det tonala ljudet i vissa situationer kan uppfattas som störande. Därför är det av intresse att kunna studera och minska på ljudnivån från en elekrisk drivlina. Målet med detta examensarbete är att hitta en effektiv metod som baseras på finita-elementmetoden (FEM) för att kunna studera ljudnivån från en elektrisk drivenhet genom att använda den kommerciella programvaran Abaqus.

Numeriska metoder för akustiska problem används i Abaqus, detta möjliggörs genom att koppla den elektriska drivlinan till den omgivande luften. Det finita-elementproblement löses sedan med en *direct-solution steady-state dynamic analysis*. Ljudnivån kvantifieras med ljudtryck, ljudintensitet och ljudeffekt och presenteras i decibelskala (dB). För att verifiera den framtagna metoden skapades en monopol, även kallad en punktljudkälla, i form av en sfär. Syftet med monopolen var att med en förenklad geometri av den elektriska drivenheten kunna jämföra ljudtrycket från simulering med teoretiska värden. Därigenom verifieras även att kopplingen mellan struktur och luftmedium modellerats korrekt.

En annan viktig del av finita-elementmodellen är randvillkoren som därför behöver verifieras. De akustiska randvillkoren modellerades på två olika sätt, först med en icke-reflekterande och heltäckande sfär runt drivenheten, och sedan med en halvsfär med ett totalreflekterande golv under. Grundläggande akustik säger att ljudeffekten från drivenheten skall vara densamma för båda modellerna, vilket visade sig stämma efter simuleringar i Abaqus.

En av slutsatserna som drogs var att den kommerciella programvaran Abaqus lämpar sig väl för att utföra simuleringar med en fluidstrukturinteraktion. En direkt- och en modalbaserad metod utvärderades med slutsatsen att den direkt-baserade metoden är mer tillförlitlig, främst i de högre frekvenserna.

Preface

This Master's thesis is to cover 20 weeks during the spring term 2022 and is a part of the Applied Mechanics programme at Chalmers University of Technology. The thesis is conducted at Volvo Group Trucks Technology (VGTT) and AFRY.

I would like to express my sincere gratitude to the people who gave me the great opportunity and made it possible to work with this thesis – thank you Anders Frid (AFRY), Maria Petersson (VGTT), Martina Andersson (VGTT), Sven Norberg (VGTT), and my examiner Håkan Johansson (Chalmers).

A special thanks to my supervisors, Anders Frid, Martina Andersson, and Sven Norberg who have provided me with knowledge and guidance throughout the thesis. Thanks to the expertise of Anders Frid within the field of acoustics, I had the possibility to explore this field and always received valuable supervision that motivated me to learn more about acoustics. Martina Andersson and Sven Norberg always provided me with clear explanations about the model I was working with and gave me great advice when working in ANSA and Abaqus.

During these 20 weeks, I had the chance to meet and work with two teams at AFRY and Volvo Group Trucks Technology and would also like to thank them for a warm welcoming into their respective work environments.

The author, Gothenburg, May 2022

Table of Contents

List of Figures

List of Tables

1. Introduction

This Master's thesis deals with the noise emission from an electric drive unit (EDU) of an electric truck during excitation. In the following sections, an introduction is given about why it is interesting to study the noise emission from an electric driveline, the approach and also what the goal is with this thesis.

1.1. Background

Future products of Volvo Group Trucks Technology (VGTT) need to fulfil a new European noise regulation that shall come into operation in 2027. Thus, a crucial task for truck manufacturers is to reduce the noise emission due to strong requirements from the society. To also meet the climate challenges and have a sustainable transport in both urban and rural environments, one change has been to switch from conventional drivelines to electric drivelines. The noise from electric vehicles has the potential to differ from the noise arising from internal combustion vehicles seen from the perspective of frequency content and sound pressure level [1]. Electric vehicles have a more tonal noise and lower sound level compared to vehicles with combustion engines that have a broad-spectrum noise. Thus, the transmission for electric vehicles contributes more to the total external and in-cab noise than in a truck with a conventional driveline [2]. Consequently, the noise that stems from the transmission is of importance and critical to understand for pass by requirements but also for the in-cab comfort, since some noises can be perceived as disturbing.

In an overall description, a heavy truck can be divided into chassis, driveline, and cab. All these subsystems need to interact with each other for an increased comfort and efficiency. In this study the focus is on the electric driveline which among other components consists of electric motors and a gearbox.

1.2. Approach

To obtain the noise emission from an electric drive unit, two main approaches are possible, experimental and computer aided engineering (CAE). This thesis focuses on simulations and the problem to be solved is a forward-coupled structural-acoustic problem. By coupling a structural domain with an exterior acoustic domain, quantities as sound pressure, sound intensity and sound power can be extracted so that the noise emission of an electric drive unit during excitation can be analysed in a simulation setting.

The numerical acoustic-structural calculation method is based on finite element method (FEM) which is the main method for solving complex engineering problems within dynamics at VGTT. However, it can be of interest to point out that there are other methods as well for solving a forward-coupled structural-acoustic problem. Examples of two other possible methods are boundary element method (BEM) and statistical energy analysis (SEA) [3]. In brief, BEM compared to FEM, requires only the boundaries as data input, i.e., the mesh is

located on the boundaries of a domain. SEA has another approach which is dividing the whole system of interest into subsystems and models the sound transmission using power balance equations. More on BEM and SEA can be found in [3].

1.3. Goal and Objective

The goal of this thesis is to develop a method to simulate the noise emission from an EDU with a given excitation applied on an adapted FE-model. The maximum run-time of a simulation should be about $8 - 12$ hours on cluster, i.e., running overnight. Thus, the size of the model and the frequency range are limited. Further, linear and logarithmic frequency resolution are studied.

The main objective of this study is to answer the following question:
Is it possible to perform a forward-coupled structural-acoustic analysis of an EDU to study the noise emission of the adapted FE-model using the commercial software Abaqus?

2. Theory

Under this section, a brief overview about acoustics is given in terms of sound definition, different acoustic quantities, near field and far field, monopole source, one-third octave band, and the acoustic wave equation.

2.1. Definition of Sound

Sound can be described as a pressure wave created by a vibrating source/object and for this definition it is assumed that the propagation is occurring through a fluid. Let assume that the surrounding medium is air, i.e., the air molecules are set in vibrational motion from the vibrating source. What happens is that the air molecules are oscillating about their equilibrium states. From the vibrating source, it is the wave motion that propagates and not the molecules. Once this wave motion is interpreted by the hearing organs, it is called sound [4].

In this study the surrounding medium around the EDU is air (specific material properties are given in Section 3.2). For air, like other fluids, the sound waves are longitudinal. Thus, the direction of the wave propagation and the direction of the vibrating motion of the air molecules is the same [5]. An illustration of a sinusoidal longitudinal wave can be seen in Figure 2.1. For a periodic longitudinal wave, compression and rarefaction occur. Shortly described, at start, the vibrating source will accelerate the adjacent air molecules forward, i.e., compression, but when the source reverses its motion, the air molecules will be accelerated backward, i.e., rarefaction occurs. Further reading on sound propagation through gas can be found in [5].

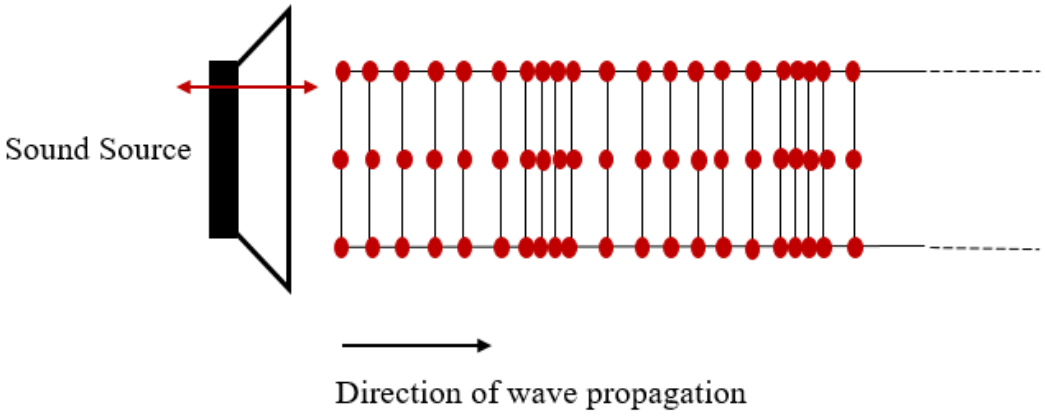

Figure 2.1: Illustration of a sinusoidal longitudinal wave. Adapted from [4].

When a sound wave is moving with a certain velocity,c, it can be characterized by its frequency or wavelength. The wavelength, λ, can be seen as the closest distance between identical parts of the wave. The frequency, f, is defined as the number of waves that pass a point per unit time and is the same as the source frequency [6]. An illustration of the wavelength of an arbitrary sinusoidal wave can be seen in Figure 2.2.

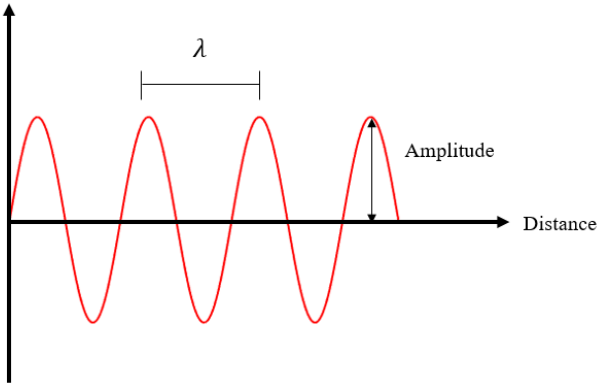

Figure 2.2: Sinusoidal wave with arbitrary frequency value and amplitude, illustrating the wavelength.

The wavelength can be calculated for different cases, which is mathematically defined as the following expression [5]:

$$\lambda = \frac{c}{f} \tag{2.1}$$

where the unit of wavelength is meter [m], f is the frequency with unit Hertz [Hz] which can also be seen as cycles/second and c is the speed of propagation of the sound wave having the unit meter/second [m/s].

2.2. Monopole Source

A monopole source is a spherical vibrating source where the sound radiates equally in all directions. For this thesis, the advantage of modelling a monopole source is that the method employed for the forward-coupled structural-acoustic problem can be verified with a simple geometry where theoretical values for pressure amplitude can be calculated. When modelling the monopole source, its geometry consists of a vibrating sphere surrounded by a spherical acoustic domain. Let the monopole source be a spherical structure that expands and contracts harmonically due to an applied pressure load inside the structure. An illustration of the monopole source can be seen in Figure 2.3.

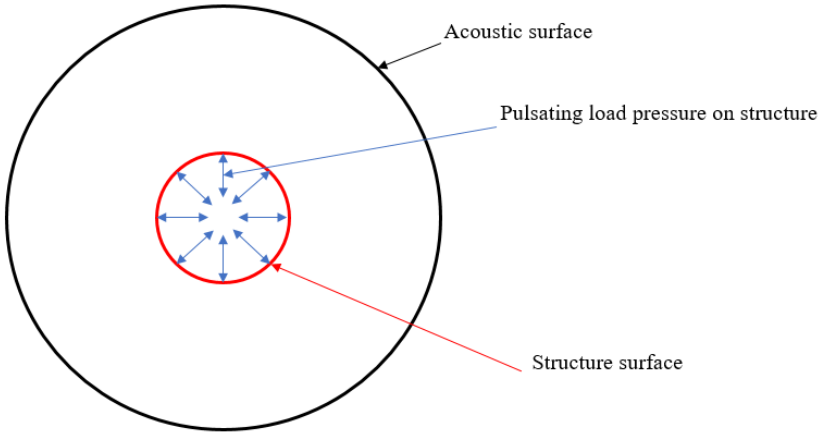

Figure 2.3: Illustration of a monopole source.

For the case in Figure 2.3, a theoretical value for the pressure amplitude can be obtained using the following equation [7]:

$$|p| = \frac{Q\rho ck}{4\pi r} \tag{2.2}$$

In equation (2.2), Q is the source strength which is the product of the surface area of the structure and the normal surface velocity of the structure, ρ is the density of air, c is the speed of sound in air, k is the wave number and r is the distance between source and the point of observation. Further, for a monopole, the sound that leaves is omnidirectional with constant source strength. To ensure that the structural sphere is a monopole source, the inequality $ka \ll 1$ needs to be fulfilled, where $k = \frac{2\pi}{\lambda}$ is the wavenumber and a is the radius of the structural sphere [7].

The monopole source is used to verify the coupling between the structure and the acoustic domain by comparing the pressure amplitude from simulation to a theoretical value using equation (2.2). By creating a vibrating structure with spherical shape surrounded by spherical acoustic domain, the monopole source is representing the EDU surrounded by air, but with a shape that allows for comparison with theoretical values. The results can be seen in Section 4.3.1.

2.3. Acoustic Quantities

In this section, a couple of different acoustic quantities are introduced. These quantities will then be used when further analysing results obtained from the FE-analysis.

The hearing of an average human is in the range of approximately 20 µPa and 20 Pa, where the lower value is the threshold of starting to hear and 20 Pa is the limit of pain [8]. Since it is a magnitude of order 10^6 between the lowest and highest limit, it is common to use logarithmic scales for acoustic quantities. The used unit when employing 10 base logarithmic scale is decibel dB where the quantity inserted into the logarithmic expression is the ratio relative to a reference value, see, for instance, equation (2.6).

2.3.1. Sound Pressure Level (SPL)

Let assume that the wave propagation is continuous, i.e., the sound is assumed to exist during long time. Thus, a root mean square (rms) acoustic pressure, p_{a_rms} can be defined from obtained acoustic pressure. From [8], the expression for p_{a_rms} is defined as the following:

$$p_{a\_rms} = \sqrt{\frac{1}{T}\int_{t_0}^{t_0+T} p_a^2 dt} \tag{2.3}$$

where T is the period time and t_0 is a fixed time.
The sound pressure level, SPL, measured in dB, is defined as the following [8]:

$$SPL = 20 \log_{10}\left(\frac{p_{a_{rms}}}{p_{a_{ref}}}\right) \tag{2.4}$$

with $p_{a\_ref} = 20$ µPa.

In Abaqus, the complex-valued acoustic pressure $\tilde{p}$ is obtained. The root mean square of the acoustic pressure is then obtained from the following expression [9]:

$$2p_{a\_rms}^2 = Re\{\tilde{p}\}^2 + Im\{\tilde{p}\}^2 \tag{2.5}$$

Expression (2.5) can be rewritten as:

$$p_{a\_rms}^2 = \frac{1}{2}(Re\{\tilde{p}\}^2 + Im\{\tilde{p}\}^2) \rightarrow p_{a\_rms} = \frac{Magnitude\{\tilde{p}\}}{\sqrt{2}}$$

The obtained p_{a_rms} can then be inserted in equation (2.4) for calculation of the sound pressure level.

The sound pressure level can be calculated in terms of the pressure magnitude as well, which can be seen in equation (2.6).

$$SPL = 20 \log_{10}\left(\frac{p_{mag}}{p_{a_{ref}}}\right) \tag{2.6}$$

Something that needs to be remarked is that the value of the sound pressure level is dependent on the position and thus the distance the sound is observed at relative to the excitation source [10]. Thus, when comparing measurement data with simulations, it is important that both the location and the distance from the sound source are the same when comparing sound pressure level.

2.3.2. Acoustic Intensity and Sound Power

In addition to acoustic pressure and sound pressure level, two more quantities are of interest in this study: acoustic intensity and acoustic power.

As it is defined in [8], the acoustic intensity can be obtained by taking the product of the acoustic pressure, p_a, and the acoustic particle velocity, $\boldsymbol{v}_a$, as:

$$\boldsymbol{I}_a = p_a \boldsymbol{v}_a \tag{2.7}$$

The unit of the acoustic intensity is W/m^2. Accordingly, acoustic intensity is the flow of sound through a unit area.

Further, the sound power, P_a with unit W, can be obtained by integrating the acoustic intensity of a closed surface, Γ. This is defined as [8]:

$$P_a = \oint_\Gamma \boldsymbol{I}_a \cdot \boldsymbol{n}\, ds \tag{2.8}$$

Here, $\boldsymbol{n}$ is the unit normal vector perpendicular to the closed surface Γ.
Moreover, sound power level, L_w can be calculated in a similar way as sound pressure level [8]. This can be seen in equation (2.9).

$$L_w = 10 \log_{10} \frac{P_a}{P_{a,ref}} \tag{2.9}$$

In contrast to sound pressure level, the sound power level is independent of position and distance from the sound source [10]. This means that sound power is a property of the studied object regardless of the room the vibrating object is placed in. This can be worth to keep in mind when reviewing results, such as in Figure 4.7, where the sound power level is obtained from an infinite boundary at three different distances from the electric drive unit. As discussed above, the obtained sound power level is theoretically expected to be equally large for all three simulations.

2.4. Near Field and Far Field

Depending on the distance from a sound source, the sound waves are having different behaviours. Near field and far field are two concepts that can be used to describe the acoustic field around a sound source. In the near field, which is defined to be at approximately one wavelength from the sound source, the sound waves are having an unpredictable and complex behaviour. What is happening near the sound source is that the sound energy circulates without propagating away [11]. Approaching a distance of one wavelength, the motion of the sound energy is both circulating and propagating which means that there is no exact relationship between distance and sound pressure [11].

In contrast to near field, the far field sound pressure level decreases with 6 decibels (dB) when doubling the distance from the sound source with the assumption that no reflection of the sound waves is present. The far field region is starting at about one wavelength and further away from the sound source. Further, in this region the acoustic pressure and acoustic particle velocity are in-phase [11].

2.5. One-Third Octave Band

To capture the overall behaviour in frequency domain of a varying sound pressure level, it is possible to use one-third octave band representation and some results will be presented in this type of representation.

An octave means a doubling of a frequency, more specifically, in an octave band, the upper frequency is twice the lower frequency [4]. For instance, there is one octave between 500 and 1000 Hz. One-third octave band is thus one-third of an octave band in a logarithmic scale.

Usually, the centre frequencies of the one-third octave band are standardised, some examples can be seen in Table 2.1 where both the centre frequencies are given and lower and upper frequency value of a one-third octave band.

Table 2.1: Standardised center frequency of a one-third octave band with its lower and upper frequencies. Adapted from [4].

Center frequency [Hz]	One-third octave band lower - upper frequency [Hz]
...	...
500	447 - 562
630	562 - 708
800	708 - 891
1000	891-1120
1250	1120 - 1410
1600	1410 - 1780
2000	1780 - 2240
2500	2240 - 2820
3150	2820 - 3550
4000	3550 - 4470
…	…

A chosen frequency range can thus be divided in several one-third octave band, where the quantity of interest between the frequencies in the band is summed. This provides a value for each centre frequency in the one-third octave band. The frequency range is divided logarithmically so that it is equally many frequencies in each one-third octave band.

2.6. Acoustic Wave Equation

To become familiar with the fundamental parts of the acoustic wave equation, an insight is given in this section of the equations defining linear acoustics. The basis behind deriving the linear acoustic equations is the fundamental equations of fluid dynamics. For further reading on mass, momentum, energy conservation equations and the constitutive equations of fluid dynamics, see [8].

The made assumptions when deriving the linear acoustic equations, are that the total variation of the entropy is zero and the pressure is assumed to be only a function of the density. Furthermore, the fluid is assumed to be non-viscous, and no external force density is considered. Combining the fundamental equations of fluid dynamics together with the made assumptions, the following equations are the starting point for deriving the linear acoustic equations [8]:

$$\frac{\partial \rho}{\partial t} + \nabla \cdot (\rho \boldsymbol{v}) = 0 \tag{2.10}$$

$$\rho \frac{\partial \boldsymbol{v}}{\partial t} + \rho \boldsymbol{v} \cdot \nabla \boldsymbol{v} + \nabla p = 0 \tag{2.11}$$

$$\frac{dp}{dt} = c^2 \frac{d\rho}{dt} \tag{2.12}$$

where p is pressure, ρ is density, $\boldsymbol{v}$ is the velocity vector, t is time and c is the speed of sound. Equation (2.12) is pressure-density relation for an isotropic state and is assumed to be satisfied by a function c_0 which is independent of t.

There are two types of acoustic boundary conditions that are used in this thesis. The first one is a total reflection of the acoustic boundary and is a Neumann boundary condition as follows [8]:

$$\frac{\partial p_a}{\partial \boldsymbol{n}} = 0 \tag{2.13}$$

In equation (2.13), p_a is the acoustic pressure and $\boldsymbol{n}$ is the unit normal vector. The second acoustic boundary condition is a homogeneous Dirichlet boundary condition (non-reflective) and is as follows [8]:

$$p_a = 0 \tag{2.14}$$

If considering the static case, it gives that the mean velocity, $\boldsymbol{v}_0$ is zero and the mean pressure and mean density are defined as, p_0 and ρ_0, respectively. For the non-static case, let a perturbation of the mean quantities be included. As given in [8], the expression becomes:

$$p = p_0 + p_a \tag{2.15}$$

$$\rho = \rho_0 + \rho_a \tag{2.16}$$

$$\boldsymbol{v} = \boldsymbol{v_a} \tag{2.17}$$

where p_a is the acoustic pressure, ρ_a is the acoustic density and $\boldsymbol{v}_a$ is the acoustic particle velocity. Further, the following relations applies as well: $p_a \ll p$ and $\rho_a \ll \rho$. Inserting equations (2.15) – (2.17) into equations (2.10) – (2.12) together with the assumption that the mean pressure does not vary over space and all second order terms are cancelled i.e., terms as, for instance, $\rho_a \boldsymbol{v}_a$, the following equations are obtained [8]:

$$\frac{\partial \rho_a}{\partial t} + \nabla(\rho_0 \boldsymbol{v}_a) = q_{ma} \tag{2.18}$$

$$\rho_0 \frac{\partial \boldsymbol{v}_a}{\partial t} + \nabla p_a = \boldsymbol{q}_{mo} \tag{2.19}$$

$$\frac{\partial p_a}{\partial t} = c_0^2 \left(\frac{\partial \rho_a}{\partial t} + \boldsymbol{v}_a \cdot \nabla \rho_0 \right) \tag{2.20}$$

q_{ma} and $\boldsymbol{q}_{mo}$ are possible source terms, representing linearized conservation of mass and linearized conservation of momentum, respectively. By inserting equation (2.18) in equation (2.20), the linear acoustic equations are obtained:

$$\frac{1}{\rho_0 c_0^2} \frac{\partial p_a}{\partial t} + \nabla \cdot \boldsymbol{v}_a = \frac{1}{\rho_0} q_{ma} \tag{2.21}$$

$$\frac{\partial \boldsymbol{v}_a}{\partial t} + \frac{1}{\rho_0} \nabla p_a = \frac{1}{\rho_0} \boldsymbol{q}_{mo} \tag{2.22}$$

Performing different mathematical operations and assuming that the speed of sound and the mean density are constant in space (for more details on the mathematical operations and assumptions see [8]), the acoustic wave equation can be expressed in terms of the acoustic pressure as:

$$\frac{1}{c_0^2} \frac{\partial^2 p_a}{\partial t^2} - \nabla \cdot \nabla p_a = \frac{\partial q_{ma}}{\partial t} - \nabla \cdot \boldsymbol{q}_{mo} \tag{2.23}$$

To express equation (2.23) in the frequency domain, Fourier transformation can be implemented, which results in the following expression [8]:

$$\nabla \cdot \nabla \hat{p}_a + k^2 \hat{p}_a = -j\omega \hat{q}_{ma} + \nabla \cdot \hat{\boldsymbol{q}}_{mo} \tag{2.24}$$

Where $\hat{p}_a$, $\hat{q}_{ma}$, $\hat{\boldsymbol{q}}_{mo}$ are Fourier transformed, ω is the angular frequency, j is the imaginary unit, k is the wave number from the wave vector defined as: $\boldsymbol{k} = k\boldsymbol{n} = \frac{\omega}{c_0}\boldsymbol{n}$ with $\boldsymbol{n}$ as the unit normal vector. For further reading on Fourier transforms, see [12].

3. Method and Numerical Model

In this section, a description about the method employed to obtain the acoustic quantities in Section 2.3 emitted from an electric drive unit (EDU) is given. Furthermore, an explanation about the numerical model is given.

3.1. Numerical Simulations in ANSA and Abaqus

The exterior acoustic domain was modelled in the pre-processor ANSA. Further, the interaction between the acoustic and the structural domain was created. Lastly, the forward-coupled structural-acoustic problem was solved in Abaqus. These topics are described in more detail in the following sections.

3.1.1. Exterior Acoustic Domain

The first step of creating the exterior acoustic domain in ANSA was to fill all holes/gaps of the electric drive unit which enables wrapping the structure by avoiding leakage. When this was done, a wrap was created around the EDU, which enables the creation of the volume mesh, i.e., acoustic domain. Depending on which frequency range is studied, the wrap mesh differs. This was calculated in ANSA with the *Acoustics Length Calculator*, where the maximum frequency of interest and how many elements per wavelength can be stated. As it is described in [9], at least six internodal intervals should be used for reasonable accuracy, and since the chosen acoustic finite element is linear, the internodal interval is the element length. For this case, it was chosen to be six elements per wavelength. An illustration of how the wrap around the EDU could look like can be seen in Figure 3.1.

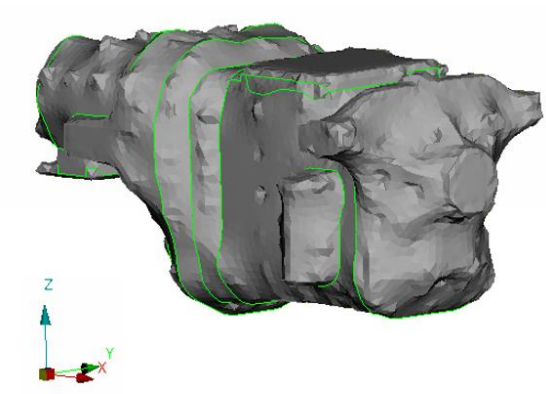

Figure 3.1: Wrap around EDU (can look differently depending on frequency range).

Once the wrap was done, a sphere was created which serves as an infinite boundary. The surface of the sphere was meshed in ANSA according to [9], more specifically the equation:

$$L_{max} < \frac{c}{n_{min} f_{max}} \tag{3.1}$$

Where L_{max} is the maximum internodal interval of an element, c is the speed of sound propagation, n_{min} is the number of internodal intervals per wavelength and f_{max} is the maximum frequency of interest. Thus, depending on the frequency range of interest, the element length is different. From [9], considering air properties, a rule of thumb for the distance between structure and surface of the exterior domain, is that it needs to be at least one-third of the wavelength at the minimum frequency of interest. A volume mesh was then created in ANSA. Since two volumes were detected, one inside the wrap and one between the wrap and the infinite boundary, i.e., the surface of the sphere, only the one between the wrap and the infinite boundary is of interest. Therefore, only the latter one is meshed with acoustic finite elements as described in Section 3.2. How the volume mesh of the sphere looks like can be seen in Figure 3.2.

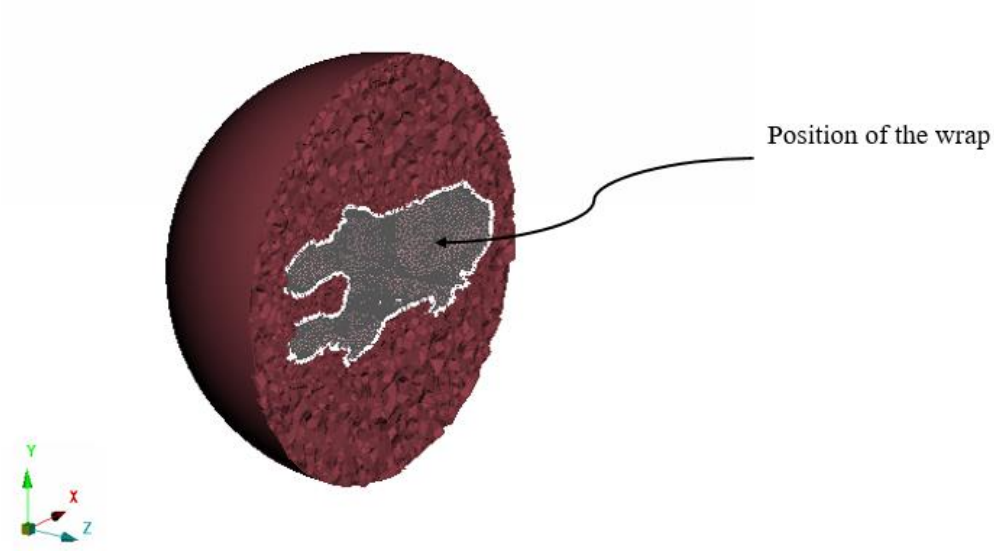

Figure 3.2: Volume mesh of the sphere cut in half around the wrap.

3.1.2. Structural-Acoustic Interaction in Abaqus

Once the exterior acoustic domain was modelled, the next step was to couple the structural domain with the exterior acoustic domain.

To ensure that the nodes on the interface, where the EDU is placed, inside the exterior acoustic domain, has the same motion as the structure, the so-called *mesh tie constraint* was used in Abaqus [13]. The structure was defined to be primary surface and the adjacent surface of the exterior acoustic domain was defined to be secondary surface, which can be seen in Figure 3.3.

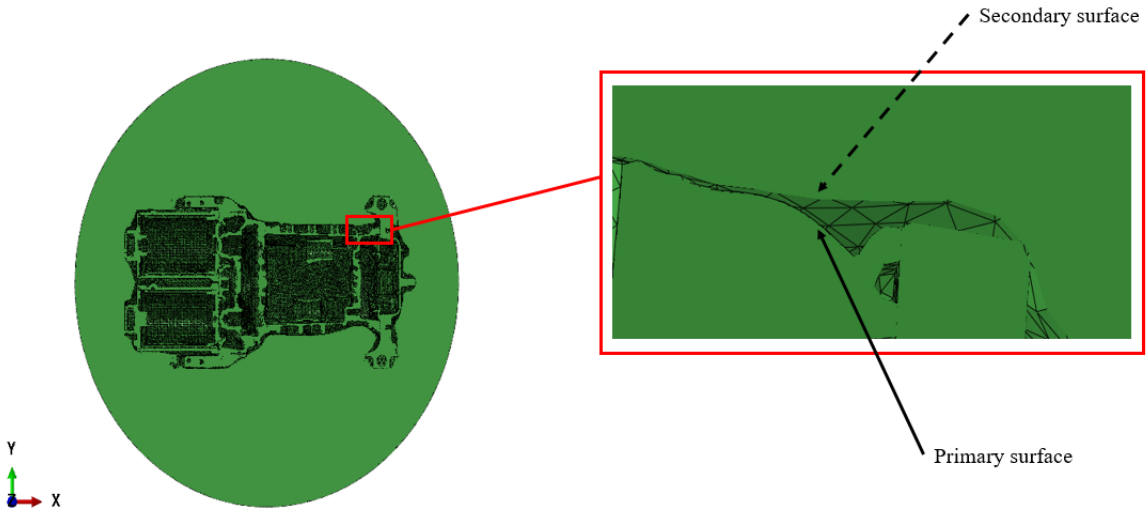

Figure 3.3: The surface of the structure is primary, and the surface of the adjacent acoustic domain is secondary.

By using tie constraint between these two surfaces, the nodes on the secondary surface were forced to have the same motion as the adjacent nodes on the primary surface.

What is happening when the surfaces are tied together is that both the tractions and the volumetric acceleration fluxes are calculated between the acoustic domain and the structural domain. The secondary surface obtains point tractions/fluxes where these are obtained by interpolation with the shape functions from the primary surface [14]. In brief, volume acceleration can be seen as an acoustic force, where the acoustic pressure is seen as acceleration [15].

A fluid-solid coupling matrix needs to be assembled, where in this case the fluid part is the acoustic domain and the solid is the electric drive unit. However, the physical degrees of freedom are different for the structural mesh and the acoustic mesh. This is considered by Abaqus, depending on which domain is defined as primary respective secondary surface. As already mentioned, the surface of the structure was defined as primary and the surface of the acoustic domain adjacent to the structure was defined as secondary surface. Thus, each node on the acoustic surface obtains an average value of the closest nodes on the primary surface. This results in displacement degrees of freedom on the acoustic surface, but since they are constrained by the primary displacements, they are eliminated [14]. The coupling condition for each node is as the following:

$$\frac{1}{\rho_f}\frac{\partial p}{\partial \boldsymbol{x}} \cdot \boldsymbol{n}^- + \ddot{\boldsymbol{u}}^p \cdot \boldsymbol{n}^- = 0 \tag{3.2}$$

where, ρ_f is the density of the acoustic medium, p is the acoustic pressure, $\boldsymbol{x}$ is the node vector on the secondary surface, $\ddot{\boldsymbol{u}}^p$ are the structural accelerations on the primary surface and $\boldsymbol{n}^-$ is the normal vector directed into the acoustic domain. Further, the fluid-structural equation coupling terms can be written as [14]:

$$\int_{\Gamma_{\text{tie}}} \delta p \boldsymbol{n}^{-} \cdot \frac{\partial p}{\partial \boldsymbol{x}} d\Gamma_{\text{tie}} = -\int_{\Gamma_{\text{tie}}} \delta p \boldsymbol{n}^{-} \cdot \ddot{\boldsymbol{u}}^{m} d\Gamma_{\text{tie}} \tag{3.3}$$

where Γ_{tie} is the interaction surface between the acoustic and structural meshes. The right-hand side term of equation (3.3) can be approximated at each node on the secondary surface, by the interpolated structural displacements values multiplied with the area of the secondary node as the following:

$$\int_{\Gamma_{\text{tie}}} \delta p \boldsymbol{n}^{-} \cdot \ddot{\boldsymbol{u}}^{m} d\Gamma_{\text{tie}} \approx A_N \left(\sum_i \ \boldsymbol{n}^{-}(\boldsymbol{x}_N) \cdot N^i(\mathbf{p}(\boldsymbol{x}_N)) \ \ddot{\boldsymbol{u}}_i{}^{m} \right) \tag{3.4}$$

Here, A_N is the area of the secondary node, $N^i(\mathbf{p}(\boldsymbol{x}_N))$ is the interpolant of the primary surface obtained at the projection of the secondary node, $\boldsymbol{n}^{-}(\boldsymbol{x}_N)$ is the normal vector directed into the acoustic domain, estimated at the secondary node. The index i indicates that the summation is over all primary nodes i, in the vicinity of the secondary node projection $\mathbf{p}(\boldsymbol{x}_N)$. This approximation is computed at each secondary node on the interaction surface and assembled into the coupling matrix.

3.1.3. Solution Steps

To solve the forward-coupled structural-acoustic problem, a steady-state dynamic analysis was employed, more specifically in Abaqus called direct-solution steady-state dynamic analysis. In this type of analysis, the steady-state harmonic response is directly calculated in terms of physical degrees of freedom. The response of the system is obtained by a harmonic excitation at a certain frequency. To obtain the desired degrees of freedom, the mass, stiffness, and damping matrices of the system are used. This analysis in Abaqus is in general computationally expensive but at the same time, more accurate than for instance modal-based steady-state dynamic analysis.

The direct-solution steady-state dynamic analysis is a perturbation procedure where the solution is obtained by linearization about a current state. It is assumed that the structure endures small harmonic vibrations about a deformed state. The equation to be solved is as follows:

$$\delta \boldsymbol{u}(\boldsymbol{M}\ddot{\boldsymbol{u}} + \boldsymbol{C}_m \dot{\boldsymbol{u}} + \boldsymbol{I} - \boldsymbol{P}) = \mathbf{0} \tag{3.5}$$

Here, $\delta \boldsymbol{u}$ is displacement variation, $\boldsymbol{M}$ is the mass matrix, $\boldsymbol{C}_m$ is the mass proportional damping matrix, $\boldsymbol{I}$ is the internal load vector and $\boldsymbol{P}$ is the external load vector. More detail on how these vectors/matrices are defined and further reformulated to obtain the stiffness matrix can be seen in [16].

Furthermore, modal-based steady-state dynamic analysis was also explored and compared with direct-solution steady-state dynamic analysis, where the results can be seen in Chapter 4.

In contrast to the direct method, the modal-based method is more computationally effective but does not provide as accurate results as the direct method. The response in the modal-based method is based on modal superposition [17].

The dynamic response of a structure when employing the modal superposition method is approximated by superposition of eigenmodes of the structure in a specific frequency range. As a first step, the eigenfrequencies need to be computed together with their respective mode shapes [18]. For a coupled structural-acoustic problem the mass, damping, and stiffness matrices can be unsymmetric which results in a more complicated procedure when employing mode superposition compared to if the matrices are real, symmetric, and positive definite. Since the principle is similar, let assume that the equation of motion for a structure consists of real, symmetric, and positive definite matrices and is described as [18]:

$$\boldsymbol{M}\ddot{\boldsymbol{u}} + \boldsymbol{C}\dot{\boldsymbol{u}} + \boldsymbol{K}\boldsymbol{u} = \boldsymbol{f}(t) \tag{3.6}$$

where $\boldsymbol{M}$, $\boldsymbol{C}$ and $\boldsymbol{K}$ is mass, damping and stiffness matrices respectively and $\boldsymbol{u}$, $\dot{\boldsymbol{u}}$, and $\ddot{\boldsymbol{u}}$ are displacements, velocities and accelerations and $\boldsymbol{f}$ is the load vector dependent on time, t. For this assumption, the obtained eigenvectors from equation (3.6) are orthogonal. Let the eigenvectors be denoted $\boldsymbol{\varphi}_i$, where i goes from 1 to n, the number of mode shapes. The eigenvectors are inserted in a modal matrix, $\boldsymbol{\Phi}$, where the rows are the number of degrees of freedom and the columns are the eigenvectors. With the modal matrix, the equation of motion can be diagonalized and transformed into decoupled second-order differential equations as the following:

$$\boldsymbol{\Phi}^{\mathrm{T}}\boldsymbol{M}\boldsymbol{\Phi}\ddot{\boldsymbol{\eta}} + \boldsymbol{\Phi}^{\mathrm{T}}\boldsymbol{C}\boldsymbol{\Phi}\dot{\boldsymbol{\eta}} + \boldsymbol{\Phi}^{\mathrm{T}}\boldsymbol{K}\boldsymbol{\Phi}\boldsymbol{\eta} = \boldsymbol{\Phi}^{\mathrm{T}}\boldsymbol{f}(t) \tag{3.7}$$

where the modal displacement is $\boldsymbol{\eta} = \boldsymbol{\Phi}^{-1}\boldsymbol{u}$. For instance, if the mass matrix is multiplied with the modal matrix, as shown in equation (3.8), the diagonal terms are called modal masses [18].

$$\boldsymbol{\Phi}^{\mathrm{T}}\boldsymbol{M}\,\boldsymbol{\Phi} = \begin{bmatrix} m_1 & 0 & 0 & 0 \\ 0 & m_2 & 0 & 0 \\ \cdots & \cdots & \cdots & \cdots \\ 0 & \ldots & 0 & m_n \end{bmatrix} = \boldsymbol{\mu} \tag{3.8}$$

Furthermore, the made assumption when using mode superposition is that the displacements can be expressed as a linear combination of the eigenmodes:

$$\boldsymbol{u}(t) \approx \sum_i^n q_i(t)\boldsymbol{\varphi}_i \tag{3.9}$$

where q_i are the modal amplitudes.

In a coupled structural-acoustic natural frequency analysis, the extracted modes have different contributions. One mode type is the so-called coupled mode, where the mode has contribution from both the structural and the acoustic domain. However, there are structural modes and acoustic modes, where most of the contribution comes from the structural respective the acoustic domain. Finally, acoustic cavity resonance modes can be present. These modes are

coupled modes with nonzero eigenfrequency that have an influence on the resulting dynamics of the acoustic pressure [9].

3.2. Mesh of the Acoustic Domain and Boundary Conditions

The acoustic domain consists of three-dimensional acoustic finite elements, more specifically, AC3D4 elements in Abaqus. This type of element is a 4-node linear tetrahedron with acoustic pressure as a degree of freedom. Furthermore, a radiating, non-reflective boundary condition was applied at the terminating surface of the sphere which means that the exterior acoustic domain is seen as wave-bearing domain, where the waves are radiating outwards the domain.

Non-reflective boundary conditions are applied in two ways to study which is preferable. The first way is by using acoustic infinite elements. In this case, the acoustic infinite elements in Abaqus are three-dimensional, 3-node linear triangular elements, ACIN3D3 with acoustic pressure as degree of freedom. An illustration of the employed acoustic finite element and acoustic infinite element can be seen in Figure 3.4. The other method of creating non-reflective boundary was to apply acoustic impedance on the surface of the acoustic domain. It was chosen to be non-reflective, i.e., the acoustic impedance is zero which gives a homogeneous Dirichlet boundary condition [8]. Acoustic impedance, Z_n is defined as follows:

$$Z_n = \frac{p}{\overline{\boldsymbol{v}_f} \cdot \overline{\boldsymbol{n}}} \tag{3.10}$$

where p is the acoustic pressure, $\overline{\boldsymbol{v}_f}$ is the fluid particle velocity and $\overline{\boldsymbol{n}}$ is the unit normal vector [8]. In other words, acoustic impedance can be seen as a measure of how easily a sound wave propagates through a fluid.

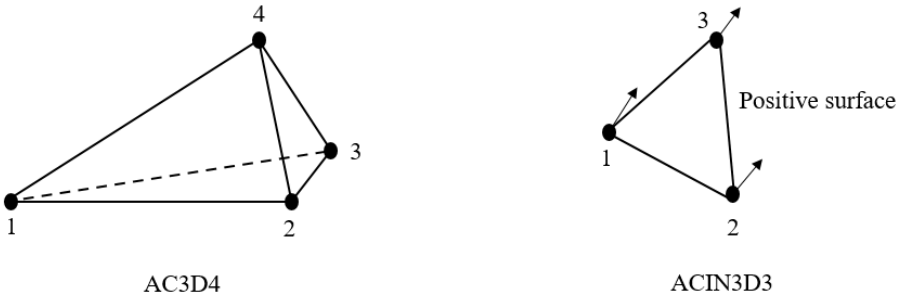

Figure 3.4: Used acoustic element types for the exterior acoustic domain. Adapted from [19] and [20].

For this thesis, a sphere was chosen to represent the exterior acoustic domain which encloses the structure, i.e., the EDU. To create the non-reflective boundary conditions, the infinite acoustic elements were applied on the terminating surface of the sphere that consists of acoustic finite elements. By applying the acoustic infinite elements on the surface, the exterior acoustic domain is seen as wave-bearing, i.e., non-reflective. For the acoustic impedance as non-reflective boundary condition, this option was chosen on the terminating surface of the sphere.

The results from employing respective method of non-reflective boundary conditions can be seen in Figure 4.2.

Furthermore, a hemisphere was also modelled as an exterior acoustic domain. The purpose with the hemisphere is to represent a semi-anechoic chamber with reflective floor. The boundary conditions of the cap of the hemisphere were the same as the entire sphere. This means that the surface of the cap is non-reflective. However, on the "ground" of the hemisphere, the boundary condition was set to be totally reflective which is a natural boundary condition. The acoustic energy reflects back into the mesh from the "ground" boundary. The type of boundary conditions applied on the sphere/hemisphere can be seen in Figure 3.5.

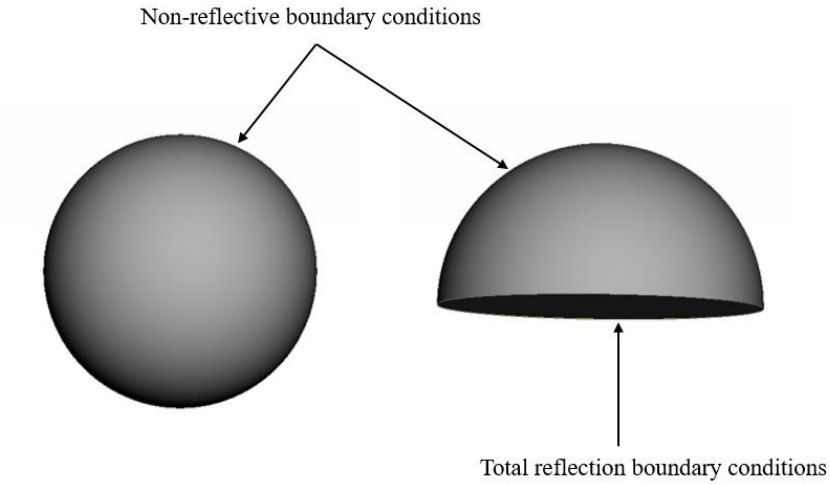

Figure 3.5: Illustration of the type of boundary condition on the surface of the acoustic domain for the sphere and the hemisphere respectively.

The material properties of the exterior acoustic domain were set to be for air within a temperature range of $5 - 25$ °C. This gives that the speed of sound is 340 m/s [8]. To obtain this speed of sound in Abaqus, the material properties were given in terms of air density and air bulk modulus. The air density was set to 1.2 kg/m^3 and the air bulk modulus was set to $1.39 \cdot 10^5$ Pa.

The FE-model of the electric drive unit was provided by VGTT with its components, material properties and mesh. The suspension of the electric drive unit is modelled with springs having different translational stiffnesses.

3.3. Load Configuration

When exploring different methods in Abaqus to find one that is efficient for calculating the noise emission from an electric drive unit during excitation, the applied load was a constant load in all three directions, i.e., the same constant load throughout the frequency range. Note that the three applied forces are in-phase. In Figure 3.6 the applied load in this study can be seen. The load was applied at a node in one of the gears of the EDU.

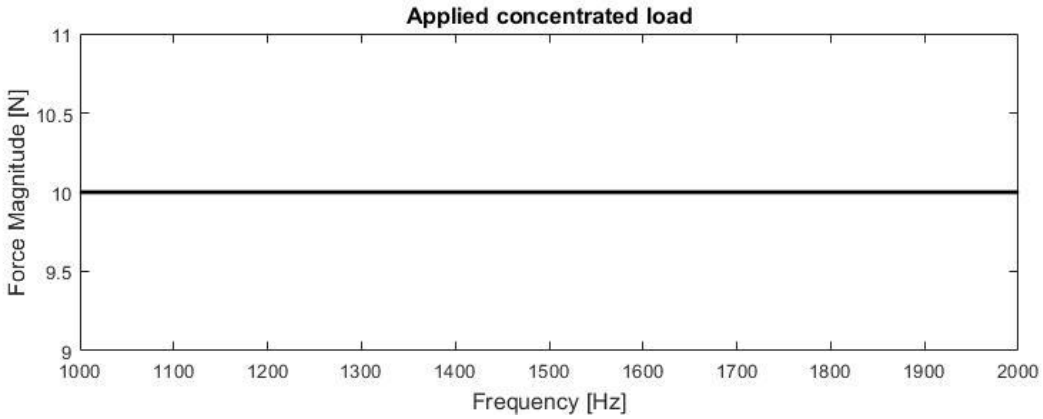

Figure 3.6: Applied constant load in the frequency domain. Here, the frequency range is $1000 - 2000$ Hz and the magnitude of the load is 10 N.

3.4. Output Data

For this study, the quantities of interest are described in Section 2.3. Thus, the same quantities were requested as output data in Abaqus where they are used for verification of the model. These can be seen in Table 3.1.

Table 3.1: Quantities of interest requested as output data in Abaqus.

Abbreviation in Abaqus	Quantity	SI - unit
POR (nodal output)	Acoustic pressure	Pa
INTEN (nodal output)	Acoustic intensity	W/m²
ALLQB (acoustic infinite element/impedance boundary)	Dissipated energy per cycle	"W/cycle" (W for sound power)

In Table 3.1, the output called ALLQB represents the dissipated energy per cycle, at all non-reflective boundaries in the frequency domain. To obtain the sound power, ALLQB is multiplied with the frequency [Hz], i.e., the dissipated energy per cycle needs to be multiplied with the frequencies in the chosen interval.

Furthermore, the acoustic intensity, INTEN, in Abaqus is given as a complex conjugation, where the real part represents active intensity, and the imaginary part represents the reactive intensity [9]. Active sound intensity can be seen as a net flow of the sound energy and the

reactive is defined as the part of the sound field where the sound energy does not have any contribution to the net sound energy flow [21]. In this thesis, only the active part was of interest since the active part of the sound intensity represents the energy that radiates out from the structure.

4. Results and Discussion

In this section, the obtained results throughout the thesis are presented and discussed. In some of the presented results, numbers are removed from the axes due to confidentiality.

4.1. Comparison Between Solution Steps

As described in Section 3.1.3, two different solution analysis were tried in Abaqus: steady-state dynamic, direct, and steady-state dynamic, modal. For the comparison between both methods, the settings for the acoustic domain can be seen in Table 4.1.

Table 4.1: Used settings for the acoustic domain for comparison of direct-solution steady-state dynamic analysis and modal-based steady-state dynamic analysis.

Acoustic Domain	
Frequency range	1000 - 2000 [Hz]
Sphere radius	850 [mm]
Longest wavelength	340 [mm]
Minimum allowable distance between structure and sphere surface	113 [mm]
Maximum element length	28 [mm]
Chosen element length on edge	50 [mm]
Non-reflective boundary conditions	Acoustic infinite elements

A coarser mesh than recommended by equation (3.1) was used in the comparison to save computational time, since the purpose of this analysis is to conclude which solution analysis to be used further on in this thesis. Employing the radius in Table 4.1, fulfills the requirement of having at least one-third of the longest wavelength between the structure and the surface of the sphere. The comparison was done by extracting the acoustic pressure at the same node on the sphere and calculate the sound pressure level for respective method. The results can be seen in Figure 4.1.

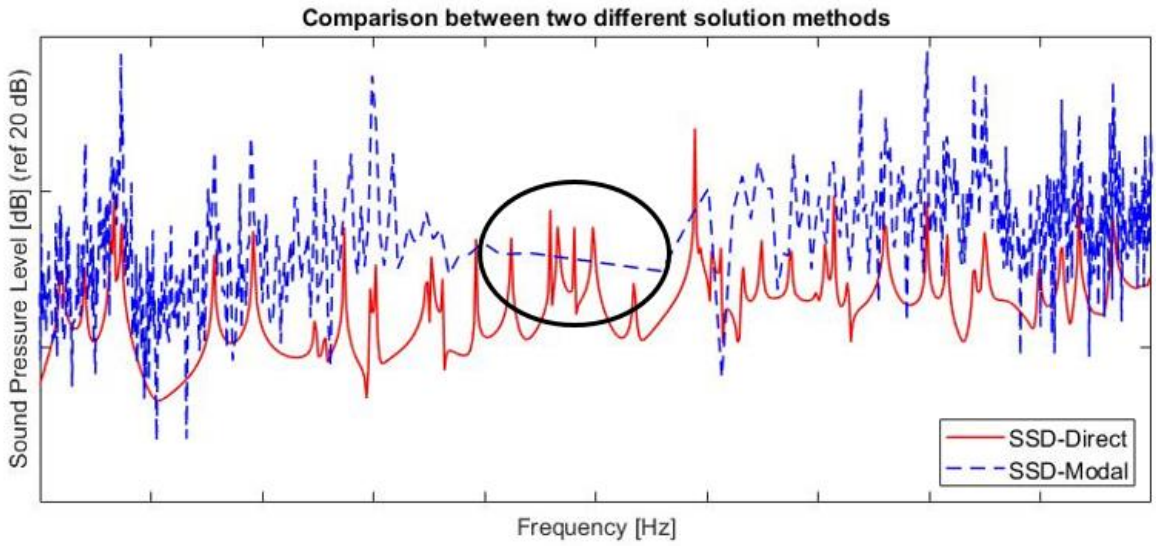

Figure 4.1: Sound pressure level at the same node for steady-state dynamic, direct (SSD-Direct) and steady-state dynamic, modal (SSD-Modal).

As can be noted in Figure 4.1, in the circumscribed area, the modal steady-state dynamic analysis shows an unnatural behavior. Furthermore, the peaks of the modal analysis are closer compared to the direct analysis, which is also a non-typical pattern for a response function. The reason for this unnatural behavior to occur for the modal analysis might be a consequence of the acoustic cavity resonance modes in combination with the applied infinite acoustic elements as a non-reflective boundary. The sharpness of the peaks for each analysis depends on that no structural damping is included during this simulation. Thus, it was concluded to continue with steady-state dynamic, direct as analysis step.

Further, the frequency range was divided linearly into 600 frequencies. By changing to logarithmically divided frequency range, the frequency resolution is remaining the same but computational time is saved. Moreover, having logarithmically divided frequency range, ensures that there are equally many frequencies in each one-third octave band.

4.2. Acoustic Infinite Elements and Acoustic Impedance

In this section, the results obtained from comparing the two types of non-reflective boundary conditions from Section 3.2 are presented. The acoustic domain is a hemisphere with a radius of $r = 1150$ mm. In the first simulation acoustic infinite elements are applied on the surface of the cap and in the second, impedance set to be non-reflective in Abaqus is applied. The frequency range is between $898 - 2818$ Hz and is divided logarithmically with in total 60 frequencies. For this interval, according to [4], there are five center frequencies: 1000, 1250, 1600, 2000 and 2500 Hz. This results in 12 frequencies that are summarized in each one-third octave band. The load is a constant unit load in the frequency range applied at the same node in respective model. The results can be seen represented in one-third octave bands in Figure 4.2 (b).

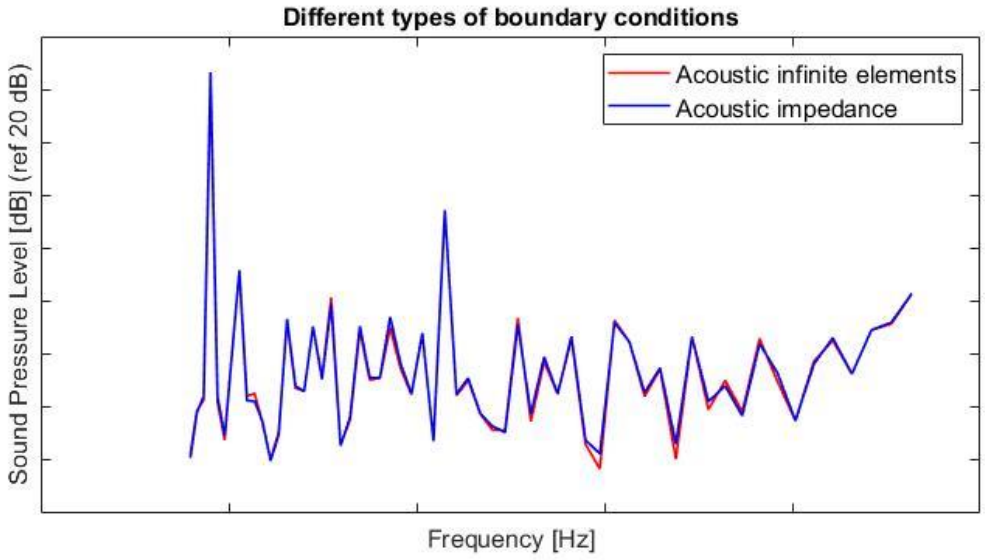

(a)

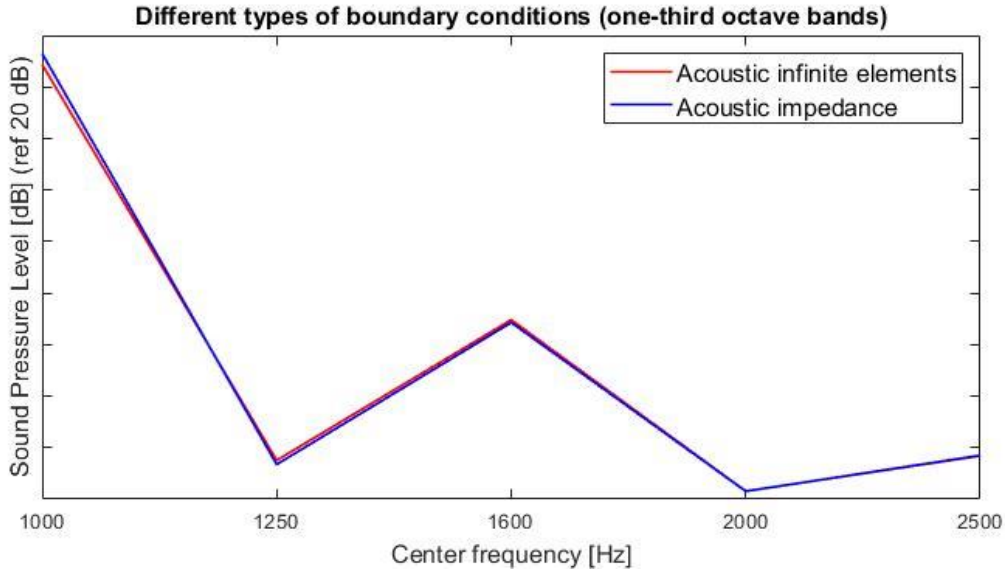

(b)

Figure 4.2: (a) Sound pressure level using acoustic infinite elements and acoustic impedance respectively, applied on the cap of the hemisphere (b) Sound pressure level using acoustic infinite elements and acoustic impedance represented in one-third octave bands.

In Figure 4.2, on the vertical axis the sound pressure level at an arbitrary chosen node (same node for both models) is seen. On the horizontal axis in Figure 4.2 (b), the center frequencies for the chosen frequency range are seen. It can be noted that both methods give the same result since the curves are lying on each other, following the same pattern. According to [9], acoustic infinite elements are more accurate than the impedance type of boundary condition, especially, for more complex features of the acoustic domain. In this case the acoustic domain has a spherical shape which results in that both methods give close to identical results.

One advantage of using acoustic infinite elements as non-reflective boundary condition is that an acoustic far-field analysis can be performed. It means that for instance acoustic far-field pressure can be computed from the infinite element sets where the results are projected on the spherical surface [22]. This facilitates the comparison with test data because the simulation can be performed fulfilling the acoustic requirements without adjusting the acoustic domain to how far away measurements have been done from the structure.

4.3. Verification of the FE-model

In this section, different methods are presented that were used to verify the finite element model.

4.3.1. Monopole source

A monopole source was created to verify that the interaction between a structure and an acoustic domain is performed properly. For this verification the model consists of a spherical shell structure with regular steel and an acoustic spherical domain with the properties of air described in Section 3.2. On the terminating surface of the acoustic domain, non-reflective boundary conditions are applied. The elements of the structure are S3R, 3-node triangular shell elements having in total six degrees of freedom per node (translation and rotation). The acoustic elements, both used for the domain and for the non-reflective boundary conditions are the same as described in Section 3.2. The goal is thus to recreate the actual problem in this work, but with a simple geometry so that the acoustic pressure can be compared with theoretical pressure values.

The frequency range for this simulation is $1000 - 5000$ [Hz] and the applied load is pressure with an amplitude of 1 MPa. A radius of 10 mm is set for the structural sphere and the radius of the acoustic domain is 400 mm, which gives that the distance between structure and acoustic surface is more than the longest wavelength that is 340 mm. The theoretical pressure amplitude using equation (2.2) at three different distances from the source is compared to respective pressure amplitude obtained from the simulation. The results can be seen in Table 4.2.

Table 4.2: Comparison of pressure amplitude between simulation and theoretical value for the monopole source at 1000 Hz.

Frequency [Hz]	Distance from the source [mm]	CAE pressure amplitude [MPa]	Theoretical pressure amplitude [MPa]
1000	400	3.90e-9	3.98e-9
1000	300	5.28e-9	5.30e-9
1000	200	8.18e-9	7.95e-9

As can be seen in Table 4.2, the theoretical and simulation pressure amplitude are similar, where it can also be noted that the closer to the monopole the observation point is, the higher the pressure amplitudes are. Using equation (2.6), the sound pressure level can be calculated at distances 200 mm and 400 mm. Since the monopole is working as a point source, doubling the distance from the source results in 6 dB reduction of the sound level [23]. Using the pressure amplitude from simulation the following is then obtained:

$$SPL_{r=200} = 20\log_{10}\frac{0.00818}{2\cdot10^{-5}} \approx 52.2 \text{ dB} \tag{4.1}$$

$$SPL_{r=400} = 20\log_{10}\frac{0.00390}{2\cdot10^{-5}} \approx 45.8 \text{ dB} \tag{4.2}$$

By doubling the distance from the monopole to the observation point, the reduction in sound level becomes $52.2 - 45.8 = 6.4$ dB, which shows that the modelling of the structural-acoustic interface works properly. This implies also that the electric drive unit should couple correctly to the acoustic domain.

For a monopole source, the pressure amplitude has the same value at a given radius from the source. This can be seen for instance at a frequency of 1000 Hz in Figure 4.3, where the pressure amplitude has the same value along the different radii.

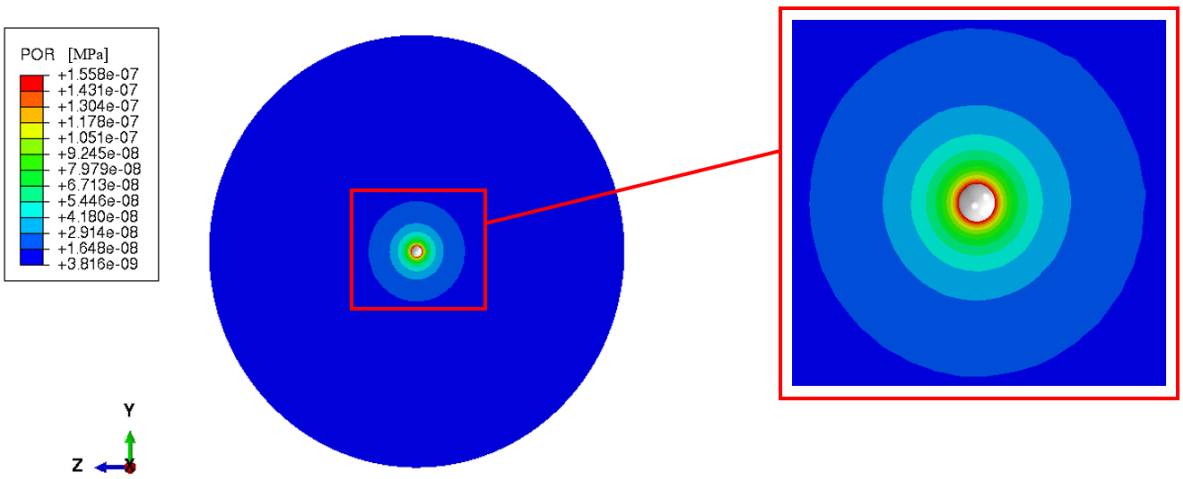

Figure 4.3: Pressure distribution at 1000 Hz.

From the zoom-in in Figure 4.3, it can be observed that the sound pressure is following an even, circular pattern centered on the source. This pattern though, is not visible for all frequencies in the chosen frequency range. For instance, at frequency 2830 Hz, the pattern starts to differ from the one seen in Figure 4.3. The pressure distribution at the cross section at 2830 Hz can be seen in Figure 4.4.

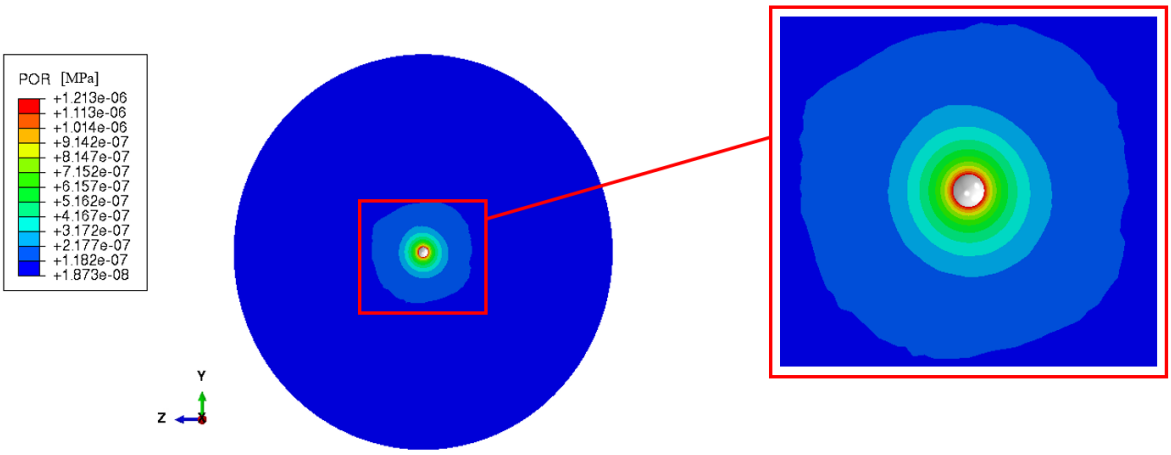

Figure 4.4: Pressure distribution at 2830 Hz.

As can be seen in Figure 4.4, the pattern around the source is starting to look more uneven compared to in Figure 4.3. This is a result of the element length of the acoustic elements. Since the acoustic elements are linear, the internodal interval is the element length. When modelling the monopole source, the chosen element length for the acoustic mesh is set to be 20 mm. From equation (3.1), having an internodal interval of 20 mm with 6 internodal intervals per wavelength, the maximum frequency becomes approximately 2830 Hz. This means that at this frequency the mesh starts to be unreliable, which can be seen in Figure 4.4 where the pattern around the monopole source is not omnidirectional.

Consequently, at a frequency of 5000 Hz, the pattern is also expected to be different from Figure 4.3, where the acoustic mesh fulfills the requirement at 1000 Hz. The pressure distribution at 5000 Hz can be seen in Figure 4.5 where it is seen that the distribution is having a chaotic pattern.

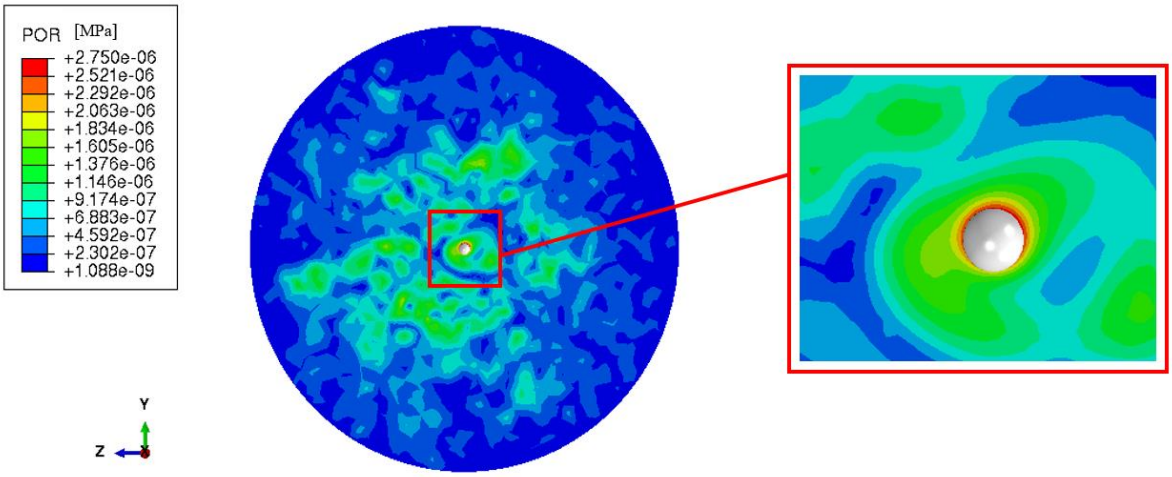

Figure 4.5: Pressure distribution at 5000 Hz.

4.3.2. Sound Power Level of a Sphere and a Hemisphere around the EDU

To verify that the applied boundary conditions of the acoustic domain are working correctly, the sound power level for a whole sphere with non-reflective boundary conditions in terms of acoustic infinite elements, and a hemisphere with a total reflection on the ground, is compared. The simulations are run with the same model of the electric drive unit. The radius of both the whole sphere and the hemisphere is $r = 1100$ mm. The boundary conditions applied for this verification can be seen in Figure 3.5. The goal is to obtain the same sound power level for the sphere and the hemisphere. For this simulation, the applied load on the EDU is as shown in Figure 3.6 and the frequency range is $898 - 2222$ Hz.

In Abaqus, the sound power was obtained by the quantity ALLQB. With some post-processing and the use of equation (2.9), the sound power level could be calculated. However, the sound power was calculated using two other methods as well, called method A and B below. Once the sound power is obtained, equation (2.9) is used and the sound power level for these methods can then be compared to the results obtained from the quantity ALLQB.

Method A is based on calculating the mean intensity of the surface of each sphere and multiply it with respective surface area. The normal sound intensity to the surface is obtained for each node on the sphere surface in Abaqus and from that the mean intensity can be calculated. For this method, the assumption is that the area of all elements on the surface of each sphere is the same. This assumption is reasonable since the elements created on the surface of the sphere are defined to have the same length.

Method B is based on the sound pressure. The sound pressure on the surface of the sphere and the hemisphere is obtained in Abaqus where the mean pressure is then calculated. Calculating the sound power is done by using the following expression:

$$W = \frac{p_{a_{mean}}^2}{c\rho} A \tag{4.3}$$

Here, W is sound power with unit W, $p_{a_{mean}}$ is the mean pressure of the sphere/hemisphere surface in unit Pa, c is the speed of sound in air in m/s, ρ is the density of air in kg/m³ and A is the surface area in m² of the sphere/cup of the hemisphere. In equation (4.3), the assumption is plane waves, i.e., the acoustic particle velocity is moving normal through the surface area.

Once, the sound power was obtained from Abaqus, Method A and B, the sound power level was calculated for the chosen frequency range. This can be seen in Figure 4.6.

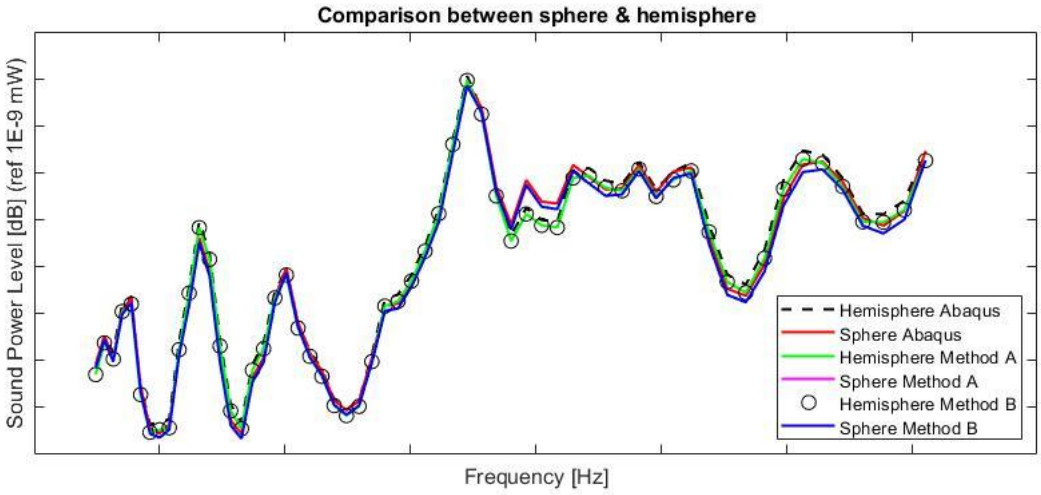

Figure 4.6: Sound power level for a sphere and hemisphere obtained by different methods.

The goal with this verification was to check that the boundary conditions are working as desired, and since the sound power level for the sphere and the hemisphere is following the same pattern in Figure 4.6, the goal is accomplished. Further, it can be noted that the results obtained from all three methods are following the same pattern at the beginning of the frequency range. As described previously, Method B assumes plane waves, which is not the real case. Thus, the results obtained from Method B are slightly different from Abaqus results and Method A at the end of the frequency range. At the middle of the frequency range, it can be seen that there is a difference between the sphere and the hemisphere, but the methods themselves are the same.

4.3.3. Different Radii of the Sphere

In this section, different radii of the sphere around the electric drive unit are compared, where all other configurations remain the same. The load is as in Figure 3.6 and the frequency range is $898 - 2222$ Hz. Three different radii of a sphere around the EDU are compared: $r = 850$ mm, $r = 900$ mm and $r = 1000$ mm. The results can be seen in Figure 4.7.

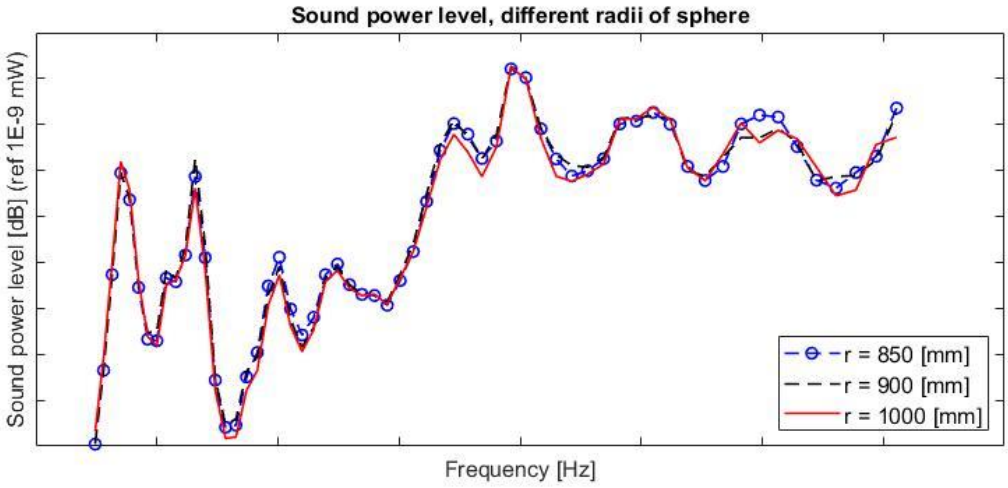

Figure 4.7: Comparison of sound power level for three different radii of a sphere around the electric drive unit.

As described in Section 2.3.2, sound power is independent of the room where the vibrating structure is placed, thus the sound power level should be the same for all three different radii of the sphere. In Figure 4.7, the sound power level for the three radii is following the same pattern which is a good indication of fulfilling the theory. However, it can be noted that at the end of the frequency range, the results for 850 mm differs from the results from the rest of the radii. Radii 900 mm and 1000 mm are following the same pattern throughout the whole frequency range. Even though a radius of 850 mm fulfills the requirement of having at least one third of the longest wavelength as a distance between the structure and the sphere, it seems that the distance needs to be longer. Thus, if comparing with test data, the acoustic domain is preferably modelled such that the distance is longer than one third of the longest wavelength.

4.4. EDU Sound Power Emission

Two models of the electric drive unit are compared, where the difference between the models is that one of the parts has different material properties. No structural damping is applied. The acoustic domain is modelled by a hemisphere with total reflection on the ground and non-reflective surface on the cap. Let call the first model of the electric drive unit for Model 1 and the second for Model 2. Model 1 has a part with higher value of the elastic modulus and density, but lower value of Poisson's ratio compared to the part in Model 2. The sound power level is compared at the same node in both models and can be seen in Figure 4.8. The frequency range for these simulations is $898 - 2818$ Hz, divided logarithmically into a total of 60 frequencies

and the results are presented in terms of one-third octave bands in a similar way as in Section 4.2.

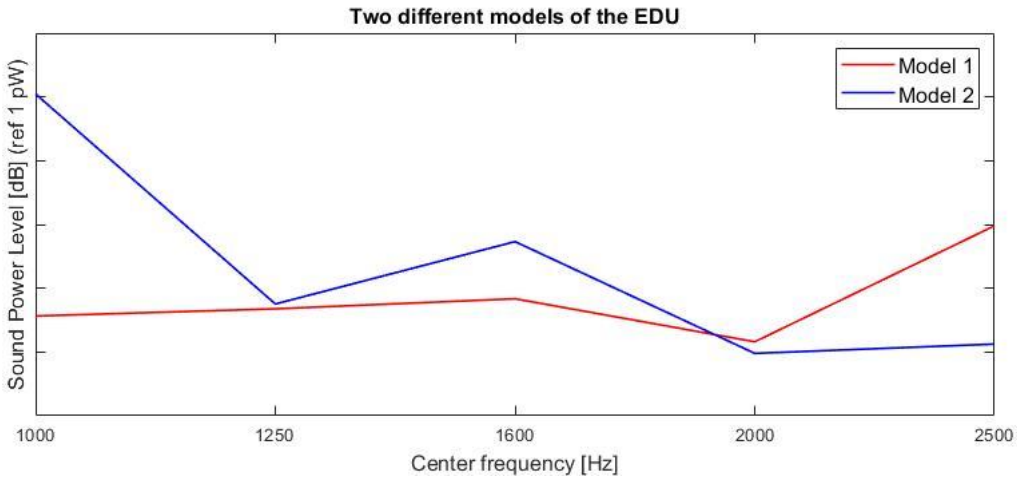

Figure 4.8: Sound power level for two different models of the electric drive unit.

In Figure 4.8, it can be seen that at the beginning of the frequency range Model 2 has higher sound power level compared to Model 1. However, at higher frequencies the sound power level becomes lower for Model 2. In this case, the load is a constant unit load with a magnitude of 1 N in the frequency domain in all three directions, since the purpose with this comparison is to obtain an overview on which design emits lower noise.

4.5. Sensitivity Study in terms of Average Sound Pressure Level

To check the sensitivity of the simulation results, a sensitivity study is performed by comparing the sound pressure level at a specific node with the average sound pressure level from a couple of nodes around at different distances. The intent of this study is to get an overview of the sensitivity of the FE-model if the simulation results are compared to test data. When comparing sound pressure level with test data, as mentioned in Section 2.3.1, the direction and the distance from the vibrating source is of importance. Thus, it is of relevance to study the sensitivity of the sound pressure level and how the results are influenced if the simulation results are gathered from nodes around the thought position of a microphone set-up.

The model for this study consists of the EDU surrounded by a hemisphere with a radius of 1150 mm. The frequency range is $898 - 2818$ Hz with 60 logarithmically distributed frequencies. Using equation (3.1) gives that the maximum allowable element length is 20 mm. Furthermore, a node is chosen on the surface of the hemisphere, which is assumed to be the exact position of a thought microphone. Around the chosen exact node, six nodes are picked at different distances, where the distances are: one element length, two element lengths, three element lengths, four element lengths and five element lengths. At each distance the average sound pressure level is calculated for the six chosen nodes. The exact node that represents a thought microphone position serves as a reference value. The nodes on the surface of the hemisphere can be seen in Figure 4.9 where the different groups are indicated by color.

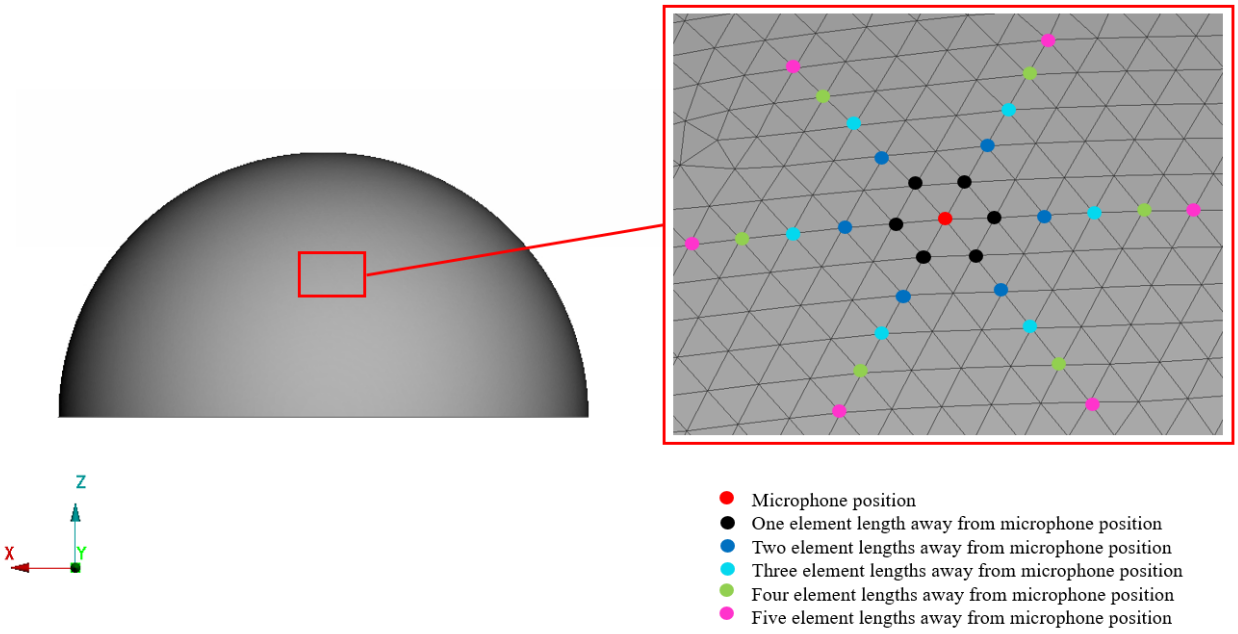

Figure 4.9: Red node in the zoom-in represents the position of a thought microphone, surrounded by nodes at five different element lengths away. One element length is 20 mm.

In Figure 4.9, the red node, is located at the middle of the EDU in x-direction, 650 mm from the structure in y-direction and 700 mm in z-direction. An average value of the sound pressure level is calculated for each node group (except the red node that is reference value), and for each frequency in the chosen frequency range. The results can be seen in Figure 4.10.

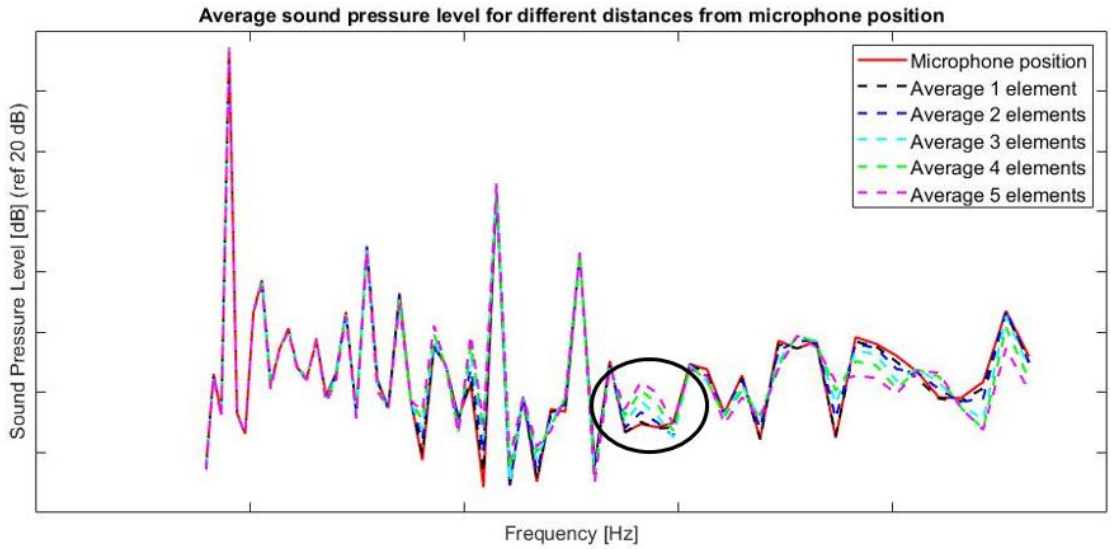

Figure 4.10: Average sound pressure level together with the sound pressure level of the chosen exact node representing a thought microphone position.

In Figure 4.10, at the circumscribed area it can be seen that the sound pressure level is deviating from the red line, the further away the nodes are from the microphone position in Figure 4.9, the larger the deviation. In general, all the curves follow the same pattern. The circumscribed area is at one particular frequency and the deviation in percentage [%] calculated in terms of sound pressure can be seen in Table 4.3. However, a deviation from the red line can also be seen at other frequencies.

Table 4.3: Deviation in percentage from the thought microphone position at a particular frequency seen as the circumscribed area in Figure 4.10.

Number of element lengths away from the microphone position	Deviation from the microphone position [%]
1	3.5
2	20
3	35
4	47
5	55

As can be noted in Table 4.3, the deviations increase with increased distance from the position of the exact node. At one element length distance from the exact node, i.e., in this case 20 mm, the deviation is around 3.5 %, which means that deviations up to one element length can be acceptable.

5. Conclusions

The commercial software Abaqus is a powerful tool allowing to solve the forward-coupled structural-acoustic problem. Performing the direct solution steady-state dynamic analysis, the exterior problem could be solved directly, without diagonalizing the equation of motion with the eigenmodes of the system. Since acoustic infinite elements are present as non-reflective boundary conditions, it was concluded that the direct solution steady-state dynamic analysis is an appropriate way of solving the acoustic exterior problem. However, the direct method is more computationally expensive compared to mode-based analysis. Thus, when running the simulations, the frequency range of interest ($898 - 2818$ Hz) is divided logarithmically into 60 frequencies so that the run time is limited to about 10 to 12 hours. Even though this frequency division gives results for one-third octave band, the frequency resolution is becoming coarser to fulfil the required run time.

Furthermore, Abaqus enables to define values of acoustic admittance/impedance for the acoustic boundary conditions, if these values are known for floor, ceiling etc. In this thesis, non-reflective boundary conditions and totally reflective boundary conditions are applied. With the case of acoustic infinite elements, far-field analysis is available which enables comparison with test data in arbitrary microphone positions.

When working in Abaqus/CAE, not all desired output quantities are available. One example is the dissipated energy per cycle through the non-reflective surface, that needs to be requested in the input file and then extracted for further post-processing so that the sound power for the whole model can be obtained. When subjecting the structure to a steady-state frequency sweep, the sound power when comparing a hemisphere and a sphere was the same which indicated that the boundary conditions were applied correctly since the results were physical.

Employing the chosen method for solving the forward-coupled structural-acoustic problem on a monopole source, the theoretical values for the pressure amplitude were consistent with those from simulation, especially further out from the sound source. Therefore, it can be concluded that the coupling between the structure and the acoustic domain is working properly together with the direct solution steady-state dynamic analysis.

From the performed sensitivity study in terms of average sound pressure level presented in Section 4.5, being 20 mm away from a chosen exact node (thought microphone position), still results in acceptable results since the deviation is limited to 3.5 % of the sound pressure level of the reference value, i.e., the exact node.

The simulation time on the cluster for the results presented in Chapter 4 is around $10 - 12$ hours. More specifically, for the hemisphere used in Section 4.5, the run-time is 12 hours and for the spheres with different radii in Section 4.3.3, the run-time is between 10 and 11 hours. The goal for the simulation time for this study is thus accomplished.

6. Future Work

Something that could be interesting to investigate further, is to study the effect on the results using other types of linear elements on the exterior acoustic domain. In this thesis, the employed elements for the exterior domain are 4-node linear tetrahedron acoustic elements. For instance, a study can be done for the different types of linear element and analyse how the element type influences the results. In Abaqus, there are several available linear acoustic element types. Aside from the one used in this thesis, other types of interest can be for instance, 5-node linear pyramids, 6-node linear triangular prisms and 8-node linear brick. For acoustic elements, the active degree of freedom is pressure. This means that changing from linear to quadratic acoustic elements, the active degree of freedom will remain the same. Therefore, a primary investigation is to study how the element type effects the results, rather than comparing the order of the elements.

In this thesis, a finite element method for solving the forward-coupled structural-acoustic problem is obtained. As a future work, it would be interesting to further investigate the model by having the operating load as excitation and compare the simulation results with test data. By using noise transfer functions (NTF), a model calibration can also be performed using test data from the specific structure. Lastly, a model validation study can be done to validate the model of the EDU and the acoustic domain.

References

[1] Marie-Agnès Pallas, John Kennedy, Ian Walker, Roger Chatagnon, Michel Berengier, et al.. Noise emission of electric and hybrid electric vehicles: deliverable FOREVER (n° Forever WP2_D2-1- V4). [Research Report] IFSTTAR - Institut Français des Sciences et Technologies des Transports, de l'Aménagement et des Réseaux. 2015, 134 p. ffhal-02177735f. Retrieved from https://hal.archives-ouvertes.fr/hal-02177735/document (2022-01-21).

[2] M. Andersson, A. Frid and S. Norberg. *FEM simulation of acoustic radiation from electric drivelines in heavy trucks – software benchmark and correlation with laboratory tests. Master Thesis Proposal, Project in Collaboration with Volvo Group and AFRY.* Gothenburg, 2021-11-01.

[3] Wang, X. (2020). *Automotive Tire Noise and Vibrations.* Butterworth-Heinemann © 2020

[4] Brunskog, J., Holmberg, D., Johansson, A-C., Nilsson, E., Sjökvist, L-G. (2005). *Grundläggande Akustik.* Lunds Tekniska Högskola.

[5] Mellow, Tim, et.al. (2012). *Acoustics: Sound Fields and Transducers.* Elsevier Science & Technology.

[6] Rice University. *17.2 Speed of Sound, Frequency, and Wavelength.* Retrieved from https://openstax.org/books/college-physics/pages/17-2-speed-of-sound-frequency-and-wavelength, (2022-02-16).

[7] Bemmen, Y.J., Russell, D.A., & Titlow, J.P. (1999). *Acoustic monopoles, dipoles, and quadrupoles: An experiment revisited.* American Journal of Physics. *67*(8), 660-664. https://doi.org/10.1119/1.19349

[8] Kaltenbacher, M. (Ed.). (2018). *Computational Acoustics.* Springer. https://doi.org/10.1007/978-3-319-59038-7 .

[9] Abaqus Inc. (2022). *Acoustic, shock, and coupled acoustic-structural analysis.* Retrieved from https://abaqus-docs.mit.edu/2017/English/SIMACAEANLRefMap/simaanl-c-acoustic.htm, (2022-02-17).

[10] SIEMENS. (2019). *Sound Pressure, Sound Power, and Sound Intensity: What's the difference?* Retrieved from https://community.sw.siemens.com/s/article/sound-pressure-sound-power-and-sound-intensity-what-s-the-difference, (2022-03-14).

[11] SIEMENS (2019). *Sound Fields: Free versus Diffuse Field, Near versus Far Field.* Retrieved from https://community.sw.siemens.com/s/article/sound-fields-free-versus-diffuse-field-near-versus-far-field, (2022-04-23).

[12] Hansen, E.W. (2014). *Fourier Transforms: Principles and Applications.* John Wiley & Sons, Inc., Hoboken, New Jersey.

[13] Abaqus Inc. (2022). *Mesh tie constraints.* Retrieved from https://abaqus-docs.mit.edu/2017/English/SIMACAECSTRefMap/simacst-c-tiedconstraint.htm, (2022-03-17).

[14] Abaqus Inc. (2021). *Surface-based acoustic-structural medium interaction.* Retrieved from https://abaqus-docs.mit.edu/2017/English/SIMACAETHERefMap/simathe-c-structacouscontact.htm, (2022-03-22).

[15] SIEMENS. (2019). *What is the acoustic quantity called Q?* Retrieved from https://community.sw.siemens.com/s/article/what-is-the-acoustic-quantity-called-q, (2022-03-22)

[16] Abaqus Inc. (2022). *Direct steady-state dynamic analysis.* Retrieved from https://abaqus-docs.mit.edu/2017/English/SIMACAETHERefMap/simathe-c-ssdyndirect.htm, (2022-05-03).

[17] Abaqus Inc. (2022). *Mode-based steady-state dynamic analysis.* Retrieved from https://abaqus-docs.mit.edu/2017/English/SIMACAEANLRefMap/simaanl-c-steadystdyn.htm, (2022-03-23).

[18] COMSOL. (2018). *Mode Superposition.* Retrieved from https://www.comsol.com/multiphysics/mode-superposition, (2022-03-23).

[19] Abaqus Inc. (2022). *Three-dimensional solid element library.* Retrieved from https://abaqus-docs.mit.edu/2017/English/SIMACAEELMRefMap/simaelm-r-3delem.htm, (2022-04-22).

[20] Abaqus Inc. (2022). *Infinite element library.* Retrieved from https://abaqus-docs.mit.edu/2017/English/SIMACAEELMRefMap/simaelm-r-infinitelib.htm, (2022-04-22).

[21] Gracey & Associates. *Sound Intensity Terms and Definitions…*Retrieved from https://www.acoustic-glossary.co.uk/sound-intensity.htm, (2022-03-30).

[22] Abaqus Inc. (2022). *Using infinite elements to compute and view the results of an acoustic far-field analysis.* Retrieved from https://abaqus-docs.mit.edu/2017/English/SIMACAECMDRefMap/simacmd-c-odbintroexaacousticfarfieldpyc.htm, (2022-04-22).

[23] Collman, R. (2015). *How Sound Reduces With Distance From a Point Source.* Retrieved from https://www.acoustical.co.uk/distance-attenuation/how-sound-reduces-with-distance-from-a-point-source/, (2022-04-11).

Department of Mechanics and Maritime Sciences
CHALMERS UNIVERSITY OF TECHNOLOGY
Gothenburg, Sweden 2022
www.chalmers.se

CHALMERS
UNIVERSITY OF TECHNOLOGY